

Yongfeng Wang, Kai Wu, Jörg Kröger and Richard Berndt

Review article: structures of phthalocyanine molecules on surfaces studied by STM

Original published in:

AIP Advances. - New York, NY : American Inst. of Physics. - 2 (2012), 041402, 10 p.

ISSN: 2158-3226

DOI: 10.1063/1.4773458

URL: <http://dx.doi.org/10.1063/1.4773458>

[Visited: 2015-01-16]



This work is licensed under a [Creative Commons Attribution 3.0 Unported](http://creativecommons.org/licenses/by/3.0/) License.
[<http://creativecommons.org/licenses/by/3.0/>]

Review Article: Structures of phthalocyanine molecules on surfaces studied by STM

Yongfeng Wang,^{1,a} Kai Wu,^{2,a} Jörg Kröger,³ and Richard Berndt⁴

¹Department of Electronics, Peking University, Beijing 100871, China

²BNLMS, SKLSCUSS, College of Chemistry and Molecular Engineering, Peking University, Beijing 100871, China

³Institut für Physik, Technische Universität Ilmenau, D-98693 Ilmenau, Germany

⁴Institut für Experimentelle und Angewandte Physik, Christian-Albrechts-Universität zu Kiel, D-24098 Kiel, Germany

(Received 22 August 2012; accepted 12 November 2012; published online 28 December 2012)

This review mainly focuses on progress recently achieved in the growth of phthalocyanine molecules on single-crystal surfaces of sub-monolayer up to few-monolayer thin films studied by scanning tunneling microscopy in our groups. On metallic surfaces such as Au(111), Ag(111) and Cu(111), molecular superstructures are determined by combining directional intermolecular interactions caused by symmetry reduction, molecule-substrate interactions and indirect long-range interactions due to quantum interference of surface state electrons. On semiconducting TiO₂ surface, molecular assembling structures are dictated by the strong molecule-substrate interaction. However, on insulating NaCl film, molecule-molecule interaction dominates over the molecule-NaCl coupling, leading to molecular growth behavior. Knowledge obtained from these studies would help people better understand the physicochemical properties of the phthalocyanine molecules at surfaces so that their new applications could be further explored and uncovered in the future. Copyright 2012 Author(s). All article content, except where otherwise noted, is licensed under a Creative Commons Attribution 3.0 Unported license. [<http://dx.doi.org/10.1063/1.4773458>]

I. INTRODUCTION

A phthalocyanine molecule is an organic macrocyclic compound with a 16-membered ring formed by alternate carbon and nitrogen. In a so-called non-substituted or metal-free phthalocyanine (H₂Pc), the molecular center consists of two hydrogen atoms. The molecular center may likewise host a metal ion through coordinating d bonds with the central nitrogen atoms. Most metal elements in the periodic table can form coordination complexes (MPc, where M stands for a metal element) with phthalocyanines. Depending on the metal ion the molecular electronic and optical properties can be tailored while leaving its overall geometric structure virtually invariant. Phthalocyanines are widely used as pigments, dyes, nonlinear optical materials, enzyme-like catalysts, liquid crystals, sensitizers in photochemical reactions or photovoltaic cells, and photodynamic reagents for cancer therapy. For some applications, the molecules need to be deposited on supporting surfaces which subsequently interact with the molecules to affect the properties of the molecules. Therefore, understanding and controlling the growth of molecular films on surfaces are of fundamental importance in bettering their performance in these applications. In this context, many important investigations into structural and electronic properties of phthalocyanines have been achieved by using various surface science techniques. While a review of this wide field is beyond the scope of this article, we list a few most recent results obtained from ultraviolet^{1,2} and X-ray^{3,4} photoelectron spectroscopy, inverse photoelectron spectroscopy,^{5,6} electron energy loss spectroscopy,⁷ near-edge X-ray absorption fine

^aE-mails: yongfengwang@pku.edu.cn, kaiwu@pku.edu.cn



structure,^{8,9} normal incidence X-ray standing waves,¹⁰ low-energy electron diffraction^{11,12} and reflection high-energy electron diffraction.¹³ In particular, the scanning tunneling microscopy (STM) has been extensively used to explore the structural and electronic features of these molecules at the submolecular level in real space.^{14–56}

There are already two excellent reviews about assemblies of phthalocyanines on surfaces.^{57,58} Nicolas Papageorgiou and co-workers presented physical aspects concerning the adsorption of phthalocyanine molecules deposited on semiconductor surfaces under ultrahigh vacuum conditions.⁵⁷ Soichiro Yoshimoto *et al.* summarized molecular assemblies of phthalocyanines and porphyrins non-covalently bounded to metal surfaces.⁵⁸ Herein we present the growth of phthalocyanine molecules on the surfaces of several conducting metals, semiconducting TiO₂ and insulating NaCl thin films under ultrahigh vacuum conditions. These studies have been performed by STM in our groups in the past several years. On Ag(111) and Cu(111), molecular superstructures are determined by directional molecule-molecule attraction induced by symmetry reduction, indirect long-range interaction due to quantum interference of surface state electrons,⁴⁸ and molecule-substrate interaction. On the cross-linked TiO₂(110)-(1×2) surface, CuPc-TiO₂ interaction dominates in molecular adsorption and assembly.⁵⁹ On NaCl ultrathin film, SnPc tilts and grows in a Volmer-Weber mode, resulting in three-dimensional molecular nanocrystals formed at the initial stage, where the molecule-molecule interaction overtakes the molecule-NaCl coupling.⁶⁰

II. CoPc ON Cu(111)

CoPc exhibits a 4-fold rotational symmetry (C_4) in vacuum. A symmetry reduction from C_4 to C_2 is observed in STM images when CoPc adsorbs onto the 3-fold symmetric Cu(111) surface (Figure 1(a)). Similarly, SnPc adsorbed on Ag(111) also shows a C_2 symmetry in STM images (Figure 1(b)). Density functional calculations - with or without van der Waals (vdW) interactions - reveal that the atomic positions in the two perpendicular pairs of molecule ligands are different for both CoPc on Cu(111)⁶¹ and SnPc on Ag(111) (Figure 1(c)). Consequently, the interaction and charge transfer between substrate and molecule should be different for the two molecular axes. The difference is highlighted by the colors marked on the ligand pairs. Green and red represent ligands along the close-packed and perpendicular direction, respectively. The green part appears as split protrusions, which corresponds to a reduced charge transfer between the substrate and molecule. In contrast, red lobes represent a large charge transfer and appear as non-split ones in STM images. The green-red cross is hereafter used to represent SnPc and CoPc with symmetry reduction.

The symmetry reduction has consequences for molecule-molecule dimers which are connected by weak C-H...N hydrogen bonds (dashed line in Figure 1(d)).^{62–65} Two different types of dimers (α and β) might be formed due to intermolecular attraction, which is induced by the aforementioned symmetry reduction (Figure 1(e)). Indirect long-range molecule-molecule interaction induced by quantum interference of surface state electrons via the substrate might lead to a third type of dimer (γ , Figure 1(e)). For SnPc-down molecules (which mean that the metal atom Sn in the non-planar SnPc molecule is in direct contact with the substrate), they prefer to form peculiar chains, where the molecular attraction between molecules occurs via split lobes (Figure 1(f), dimer α). At low coverages ($\theta < 0.5$ ML), standing wave patterns around CoPc could be observed clearly (Figure 1(g)). The surface charge density variations around CoPc molecules mediate long-range interactions among the molecules. Histograms of the nearest-neighbor separations of CoPc at low coverages show preferred distances of 2.1, 3.6, 5.0 and 6.5 nm. The 1.5 nm difference well matches half the Fermi wavelength of the Cu(111) surface state.

For a slightly higher coverage ($\theta > 0.5$ ML), a uniform compression of the intermolecular distance is not observed in experiments, a scenario indicative of direct molecule-molecule interaction such as dipole-dipole⁶⁶ or electrostatic⁶⁷ repulsion. Rather, CoPc molecules form one-dimensional chains (Figure 1(i)), indicating that the surface state is essential in the structure formation of CoPc on Cu(111). Coverage-dependent experiments suggest the sequence of binding energies $E(\gamma) > E(\alpha) > E(\beta)$. This sequence of energies is valuable for understanding self-assembly of CoPc on Cu(111). At a coverage of $\theta \approx 0.5$ ML, a long-range dispersed hexagonal pattern was formed (Figure 1(h)), where the distance between two molecules in dimer γ is 2.1 nm. This molecular pattern is similar

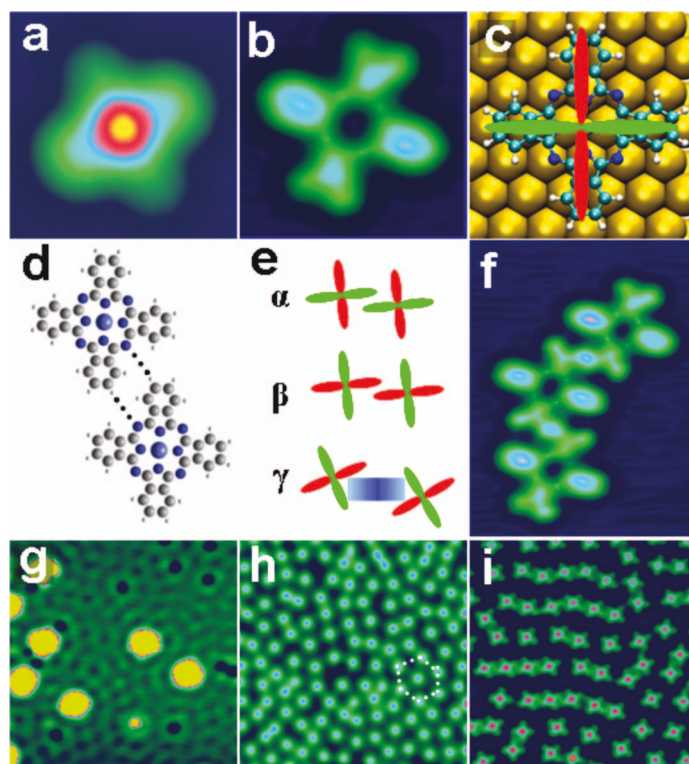


FIG. 1. Constant-current STM images of (a) CoPc on Cu(111) ($2\text{ nm} \times 2\text{ nm}$, -0.6 V) and (b) SnPc-down on Ag(111) ($2\text{ nm} \times 2\text{ nm}$, -0.03 V). Molecular lobes appear split along the $1-10$ substrate direction. (c) Relaxed geometry of SnPc-down on Ag(111). The superimposed red/green cross denotes split/non-split lobes or larger/smaller partial charge transfer between Ag(111) and SnPc, respectively. (d) Schematics of a molecular dimer with weak C-H...N hydrogen bonds. (e) Three dimer configurations. Dimer α is coupled via H-bonds, while dimer γ is stabilized by surface state-mediated interaction. Dimer β was not observed. (f) STM image of a SnPc-down trimer ($3\text{ nm} \times 4\text{ nm}$, -0.05 V) formed along the split lobes (green part of the cross). (g) STM image of standing wave patterns around CoPc on Cu(111) ($20\text{ nm} \times 20\text{ nm}$, -0.6 V). (h) 0.5 ML CoPc on Cu(111) ($25\text{ nm} \times 25\text{ nm}$, -1.0 V). Typical intermolecular distance is 2.1 nm . (i) Coexistence of dispersed molecules (predominant distance 2.1 nm) and molecular chains (interchain distance 2.1 nm , intrachain distance 1.5 nm) (0.55 ML , $16\text{ nm} \times 16\text{ nm}$, -1.0 V). The color scale bar for the STM images is shown in (f). Reprinted with permission from Y. F. Wang *et al.*, J. Am. Chem. Soc. **131**, 10400 (2009). Copyright 2009, American Chemical Society.

to Br island on Cu(111)⁶⁶ and Cu on Cu(111),⁶⁸ which are both stabilized by indirect long-range interaction induced by the Friedel-type oscillations of the local density of surface states around the adsorbates.^{69,70} Upon increasing the coverage up to 0.7 ML , an ordered array of chains is observed in STM images (Figure 2(a)), where the unique distance between two adjacent chains is again 2.1 nm . This array is composed of dimers α and γ . In dimer α , molecules are exclusively connected by green lobes. At the coverage of 0.8 ML , CoPc forms an unusual Kagome network (Figure 2(b)), which exhibits the highly symmetric plane group $p31m$. Once again, an intermolecular distance of 2.1 nm is experimentally observed, indicating that surface-state-mediated interaction plays an important role in the formation of the pattern. At 1.0 ML , CoPc forms close packed patterns in which molecules adopt two alternating adsorption configurations to reduce repulsion between red lobes (Figure 2(c)).

III. SnPc ON Ag(111)

Figure 3(a) displays two distinct images of SnPc on Ag(111).⁴⁶ While one kind of molecule gives rise to a depression (central Sn atom points towards the surface, Sn-down) at its center, the other kind exhibits a protrusion (central Sn atom points towards vacuum, Sn-up). While Sn-up molecules are isolated from each other and from Sn-down molecules as well, Sn-down molecules agglomerate and form one-dimensional (1D) chains (Figure 1(a)). The absence of SnPc-up aggregates might be due to

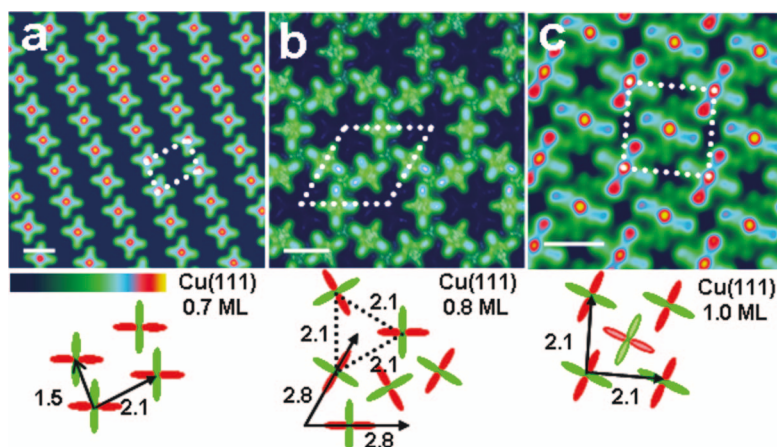


FIG. 2. STM images and schematic models of superstructure of CoPc on Cu(111). Below 1.0 ML, CoPc molecules form ordered arrays of chains ((a), 0.7 ML, -0.5 V), and a kagome network ((b), 0.8 ML, 0.2 V) on Cu(111). The color scale bar for STM images is shown in (a). At ~ 1.0 ML, CoPc assembles into a superstructure with an alternating pattern with 2 molecules per unit cell ((c), $6\text{ nm} \times 6\text{ nm}$, -0.6 V). Two simplified models with different color depths denote two different adsorption geometries in (c). White scale bars in all images denote 1.5 nm . Adapted with permission from Y. F. Wang *et al.*, J. Am. Chem. Soc. **131**, 10400 (2009). Copyright 2009 American Chemical Society.

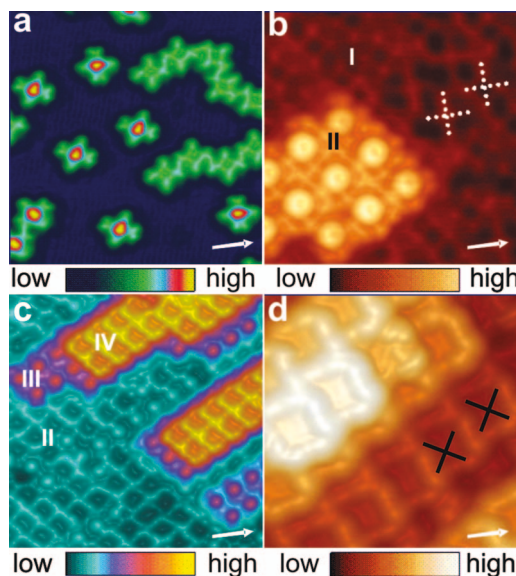


FIG. 3. Pseudo three-dimensional constant-current STM images of SnPc on Ag(111) at a) 0.2 ML ($14.0\text{ nm} \times 14.0\text{ nm}$, -0.5 V , 0.08 nA), b) 1.2 ML ($8.4\text{ nm} \times 8.2\text{ nm}$, 1.2 V , 0.1 nA), c) 2.5 ML ($17.0\text{ nm} \times 17.0\text{ nm}$, 1.4 V , 0.08 nA), and d) 6 ML ($6.9\text{ nm} \times 6.9\text{ nm}$, 2.7 V , 0.03 nA). Layer numbers are indicated by I–IV. Crosses indicate molecule positions in (b) and (d). Arrows point along the crystallographic^{1–10} direction. Adapted with permission from Y. F. Wang *et al.*, Angew. Chem. Int. Ed. **48**, 1261 (2009). Copyright 2009 Wiley-VCH Verlag GmbH & Co. KGaA.

a strong molecule-substrate interaction as was observed in CuPc on the cross-linked $\text{TiO}_2(110)-(1 \times 2)$ surface.⁵⁹ This possibility is ruled out by DFT (with or without vdW interaction) calculations, which shows a higher adsorption energy for SnPc-down molecules compared to SnPc-up ones. The central Sn atom and the Pc plane carry positive and negative charge, respectively, giving rise to a dipole moment perpendicular to the molecular plane. This dipole-dipole repulsion, together with quantum interference of the surface state electrons, exceeds the attraction between molecules originating from C-H...N hydrogen bonds. For the SnPc-down molecules, dipole moments are effectively decreased by the charge transfer between tin and the silver substrate and then the dipole-dipole

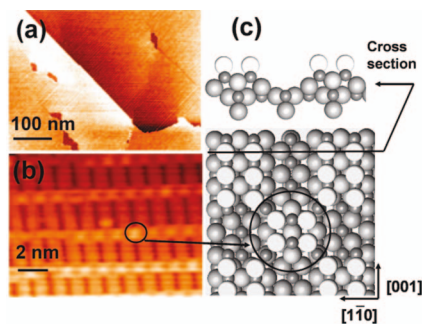


FIG. 4. (a) Large-scale and (b) high-resolution constant-current STM images of the cross-linked $\text{TiO}_2(110)-(1 \times 2)$ surface. (c) Top view and side view of the surface structural model of the cross-linked $\text{TiO}_2(110)-(1 \times 2)$. Large balls represent O atoms (anions) and small balls, Ti atoms (cations). The white balls represent the O atoms in the topmost layer. Reprinted with permission from Y. F. Wang *et al.*, J. Phys. Chem. B **110**, 17960 (2006). Copyright 2006 American Chemical Society.

repulsive interaction should be less stronger. At last, a net attraction, owing to C-H...N hydrogen bonds, remains and leads to agglomeration of the SnPc-down molecules.

For SnPc molecules in the second molecular layer, the molecule-molecule coupling dominates the molecule-substrate interaction and molecules prefer to form two-dimensional islands at low coverages (Figure 3(b)). Homogeneous islands with a single orientation (SnPc-up or SnPc-down) are formed at the initial stage due to that the SnPc molecules are quite mobile on a molecule layer at room temperature and molecule-molecule hydrogen bonds are optimized in the process.

Starting from the third layer, the growth behavior changes from 2D layer-by-layer into three-dimensional (3D) island growth (Figure 3(c)). At a coverage of 2.5 ML, a statistical analysis indicates that approximately 75% of molecules in the third layer are covered by molecules in the subsequent fourth layer. The third layer is mainly composed of SnPc-up molecules and the fourth layer consists of SnPc-down molecules. This double-layer island growth mode maintains until the coverage increases up to 6 ML (Figure 3(d)). All molecules in the topmost layer are SnPc-down molecules, with the SnPc-up ones staying in the layer underneath.

IV. CuPc ON THE CROSS-LINKED $\text{TiO}_2(110)-(1 \times 2)$ SURFACE

In general, phthalocyanines on metallic substrates are mobile at room temperature and low coverages. Structural aspects are therefore accessible by low-temperature (LT) STM only. In contrast, on TiO_2 single dispersed CuPc molecules could be imaged at room temperature.⁵⁹ TiO_2 is widely used in painting, gas sensing, photocatalysis, and dye-sensitized solar cells.^{71–73} The adsorption of CuPc on TiO_2 is worthwhile to be investigated since it represents a model system for dye-sensitized solar cells and might be useful in purification of wastewater. The $\text{TiO}_2(110)$ surface is quite complicated and its structure strongly depends on the preparation process parameters such as the annealing temperature, duration time and ion bombardment.^{74,75} The cross-linked $\text{TiO}_2(110)-(1 \times 2)$ surface is the most favorable structure and most frequently used in experiments. Large-scale and high-resolution STM images of the cross-linked $\text{TiO}_2(110)-(1 \times 2)$ surface are shown in Figures 4(a) and 4(b). Figure 4(c) shows the top and side view of the reconstructed surface structural model. This structure contains the link along $^{1-10}$ direction and Ti_2O_3 added row along the [001] direction.⁷⁶

Figure 5 shows an STM image of CuPc deposited on the cross-linked $\text{TiO}_2(110)-(1 \times 2)$ substrate. CuPc tends to locate at step edges, as shown in the inset in Figure 5. On the cross-linked $\text{TiO}_2(110)-(1 \times 2)$ terrace, there are two main CuPc configurations which have been experimentally captured. In the first configuration, CuPc locates at the link site marked by the black rectangle. It shows a typically four-lobed shape, being similar to that of CuPc on metals where CuPc lies flat on the substrates.

Figure 6(a) (top view) and Figure 6(c) (side view) show the proposed adsorption model. It is known that nitrogen exhibits a strong interaction with the 5-fold coordinated Ti sites.⁷⁷ It seems that CuPc is stabilized by the cooperative interactions between four molecular nitrogen atoms and

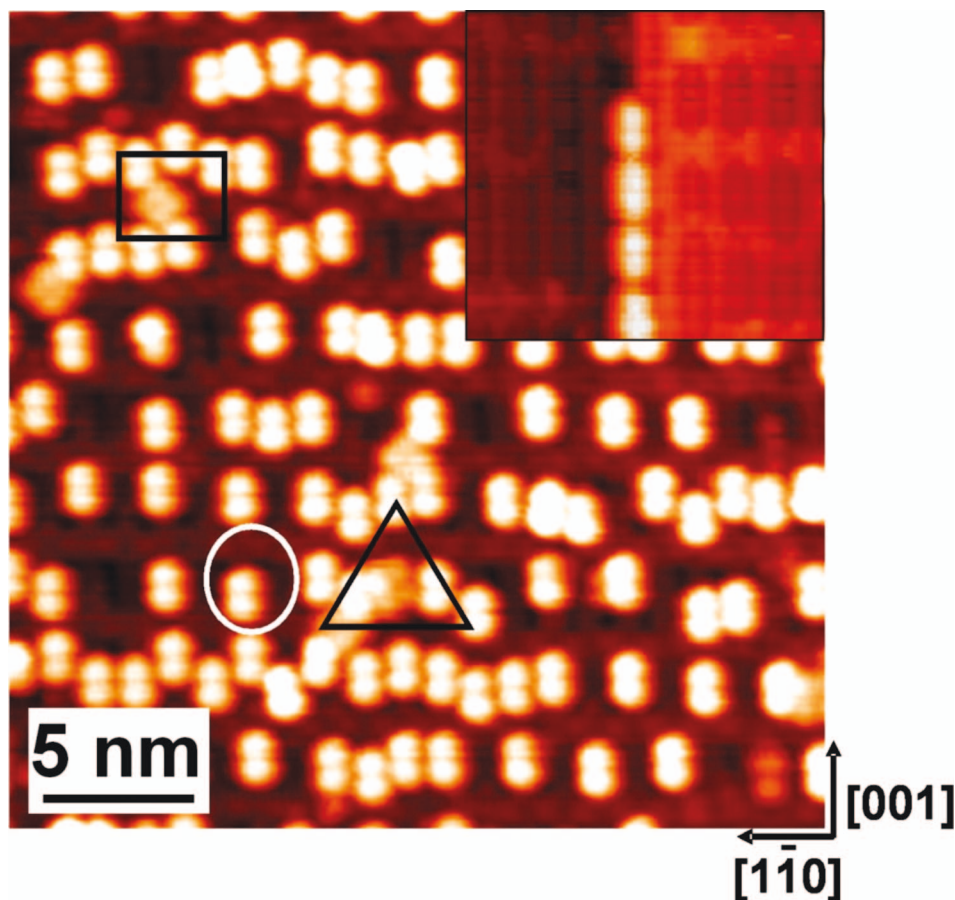


FIG. 5. Constant-current STM image of the CuPc molecules on the cross-linked TiO₂-(110)-(1×2) surface. The inset is the STM image of CuPc adsorbed at the step site. Adapted with permission from Y. F. Wang *et al.*, J. Phys. Chem. B **110**, 17960 (2006). Copyright 2006 American Chemical Society.

the underlying unsaturated Ti atoms pointed out by four thick arrows. In addition, the central Cu atom would interact with four underlying O atoms and the four indole groups would interact with underlying Ti atoms. Further stabilization may result from the interactions of two N atoms in other two rings pointing towards vacuum. The H atoms interact with the O atoms of the substrate, as marked by two thick arrows. The central Cu atom has strong interaction with two O atoms below it. Further stabilization originates from the interaction between two bridging N atoms, two nearby Ti atoms and the vdW force between the molecule and the substrate. Occasionally, a third configuration highlighted by the triangle could be observable in STM images. It is formed by rotating the CuPc molecule in Figure 5 by 45° around its 4-fold rotation axis.

V. SnPc ON NaCl DOUBLE-LAYER FILMS SUPPORTED BY Au(111)

On metals and semiconductors, phthalocyanines prefer to lie flat on the surface and grow in a layer-island (Stranski-Krastanov) mode. However, Volmer-Weber growth of molecular nanocrystals occurs when SnPc adsorbs on NaCl double-layer films supported by Au(111).⁵⁹ A constant-current STM image of Au(111) partially covered by a double-layer NaCl film is shown in Figure 7. The inset presents the schematic structure of NaCl. When deposited onto this NaCl-covered Au(111), the SnPc molecules first adsorb on the Au(111) surface. The growth behavior of SnPc on Au(111) is similar to that of SnPc on Ag(111). Once metal sites are fully occupied by SnPc, the molecules start to form the first layer on the NaCl film.

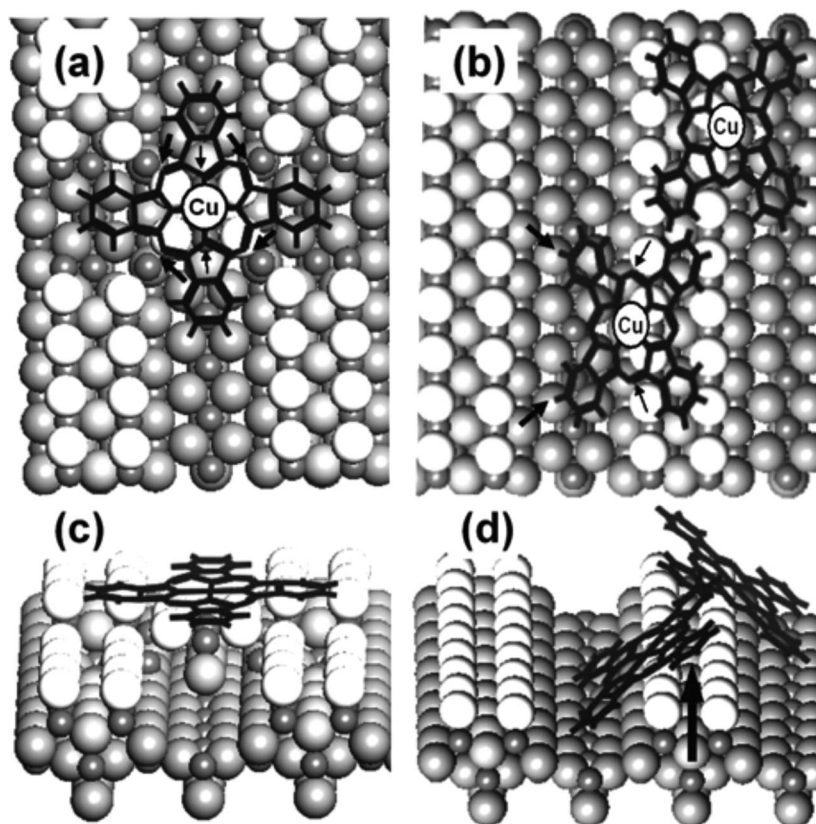


FIG. 6. Top views of the proposed structural models of CuPc at (a) the link site and (b) the added row site on the cross-linked TiO₂-(110)-(1×2) surface. Parts c and d are the corresponding perspective views of the proposed structures. In part a, the thick and thin arrows indicate possible coordination of the N atoms outside and inside the indole rings with nearby underlying Ti atoms in the substrate, respectively. In part b, thick and thin arrows indicate possible interactions of the H atoms in the benzene rings and the bridging N atoms in the N8 core with nearby O atoms and Ti atoms of the substrate, respectively. The long arrow in part d indicates the nonperfectly lined side indole rings pointing upward of two CuPc in two neighboring troughs along the [001] direction. Adapted with permission from Y. F. Wang *et al.*, *J. Phys. Chem. B* **110**, 17960 (2006). Copyright 2006 American Chemical Society.

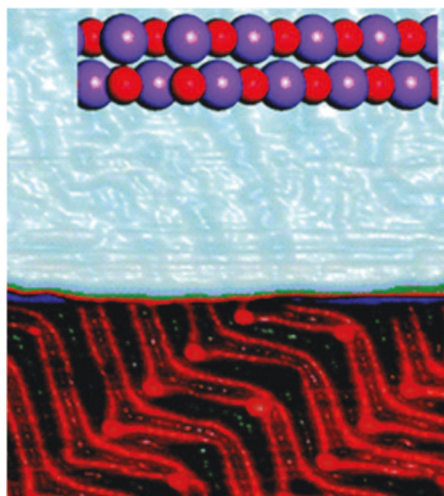


FIG. 7. STM image of Au(111) partially covered by a NaCl double layer with schematic structure as an inset (61 nm × 71 nm; −1.0 V, 0.09 nA). Adapted with permission from Y. F. Wang *et al.*, *J. Am. Chem. Soc.* **132**, 12546 (2010). Copyright 2010 American Chemical Society.

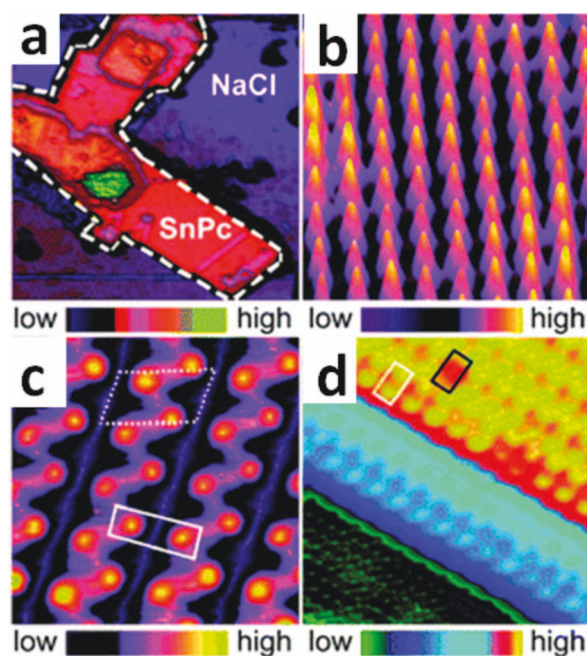


FIG. 8. Pseudo-three-dimensional representation of constant-current STM images: molecular islands of SnPc on NaCl film [a, $(62 \text{ nm})^2$; 2.2 V, 20 pA], atomic resolution image of NaCl [b, $(2.9 \text{ nm})^2$; 0.1 V, 100 pA], submolecular resolution image of SnPc nanocrystal [c, $(3.5 \text{ nm})^2$; 1.86 V, 80 pA], and high resolution image of NaCl and SnPc resolved simultaneously [d, $(8.4 \text{ nm})^2$; 2.2 V, 26 pA]. Adapted with permission from Y. F. Wang *et al.*, J. Am. Chem. Soc. **132**, 12546 (2010). Copyright 2010 American Chemical Society.

Figure 8(a) shows an STM image of SnPc nano-island. The NaCl film around the molecules is atomically resolved (Figure 8(b)). The STM images of SnPc on NaCl with submolecular resolution are given in Figures 8(c) and 8(d), where only two isoindole groups of each SnPc molecule are visible as protrusions. This observation infers that the SnPc molecules tilt on NaCl with two isoindole groups pointing towards vacuum and the other two, towards NaCl. The energetically favorable adsorption configuration as revealed by supporting calculations consists of the SnPc molecular plane inclined by 65° with respect to the surface normal of the double-layer NaCl film. This angle is in agreement with experimental observations. From the apparent height difference between subsequent molecular layers (0.5 nm) and the lateral size of a molecule (1.3 nm), an angle of $\arccos(0.5/1.3) \approx 67^\circ$ can be deduced. The dashed parallelogram in Figure 8(c) marks the unit cell in the top layer with parameters: $0.8 \text{ nm} \times 1.3 \text{ nm}$ and an angle of 71° between the unit cell vectors. A similar unit cell ($0.8 \text{ nm} \times 1.4 \text{ nm}$, 73°) was obtained by the theoretical calculation with EpiCalc. Molecular dynamics calculations indicate that the strong intermolecular interaction results in the molecular tilting within its molecular nano-crystals. Single SnPc molecule adopts a flat geometry with the molecular plane parallel to the surface.

VI. SUMMARY

Self-assemblies of phthalocyanine molecules on various substrates from sub-monolayer to few-monolayer thin films have been studied by STM in our groups. The variety of observed structures is dictated by the subtle balance between molecule-molecule and molecule-substrate interactions. On metal surfaces intermolecular coupling may be direct (e.g., dipole-dipole repulsion) or indirect (mediated by the conduction electrons). The resulting molecule assemblies (chains and two-dimensional islands) are formed owing to the rather high molecule mobility. Semiconductor surfaces tend to form strong chemical bonds to the molecule, which often results in mono-dispersed molecules. Ultrathin insulating films on metal surfaces decouple the molecules from the metal and as a result, the intermolecular interactions dominate to produce molecular nanocrystals.

Specifically, an ordered chain array and a Kagome lattice with the symmetry group $p31m$ of CoPc on Cu(111) can be prepared by combining CoPc-Cu(111) interaction, directional CoPc-CoPc attraction induced by symmetry reduction, and indirect long-range interaction caused by quantum interference of surface state electrons. For SnPc on Ag(111), two-dimensional layer-by-layer growth turns into three-dimensional island growth from the third layer on. Both SnPc-up and SnPc-down molecules coexist in the first and second layer. At higher coverages, the layers are composed of molecules with single orientation. The CuPc molecules deposited on the cross-linked $\text{TiO}_2(110)-(1 \times 2)$ surface shows four adsorption structures and their appearances in STM images are dependent on their adsorption sites. On NaCl films, SnPc-SnPc interactions prevail over the SnPc-NaCl coupling, leading to that SnPc tilts on the surface and grows in a Volmer-Weber mode.

To summarize, STM has been widely used to study at the molecular and atomic levels the structural and electronic properties of the phthalocyanine molecules adsorbed at surfaces under various conditions. Accordingly, different approaches have been developed to control the adsorption and assembly of the phthalocyanine molecules at surfaces. In the past years, rapid progress has been made to understand the adsorption behavior of the phthalocyanine molecules by employing different types of substrates. This would certainly be helpful in fine-tuning the physicochemical properties of the ensembles involving the phthalocyanine molecules, a family of very important chemical molecules that have great applications in physics and related sciences. Obviously, such studies are still far away from completeness. Continuous effort has to be made to better the performance of the phthalocyanine molecules and explore their further and new applications in all walks.

ACKNOWLEDGMENTS

This work was financially supported by the Deutsche Forschungsgemeinschaft through SFB 677, Germany, and NSFC and MOST, China.

- ¹ M. Schmid, A. Kaftan, H.-P. Steinrück, and J. M. Gottfried, *Surf. Sci.* **606**, 945 (2012).
- ² T. Hosokai, H. Machida, A. Gerlach, S. Kera, F. Schreiber, and N. Ueno, *Phys. Rev. B* **83**, 195310 (2011).
- ³ S. Lindner, M. Knupfer, R. Friedrich, T. Hahn, and J. Kortus, *Phys. Rev. Lett.* **109**, 027601 (2012).
- ⁴ K. R. A. Nishida, B. Wiggins, K. W. Hipps, and U. Mazur, *J. Phys. Chem. C* **115**, 16305 (2011).
- ⁵ H. Yoshida, *Chem. Phys. Lett.* **539**, 180 (2012).
- ⁶ F. Schmitt, J. Sauther, S. Lach, and C. Ziegler, *Anal. Bioanal. Chem.* **400**, 665 (2011).
- ⁷ W. D. Dou, S. P. Huang, R. Q. Zhang, and C. S. Lee, *J. Chem. Phys.* **134**, 094705 (2011).
- ⁸ F. Petraki, H. Peisert, U. Aygul, F. Latteyer, J. Uihlein, A. Vollmer, and T. Chasse, *J. Phys. Chem. C* **116**, 11110 (2012).
- ⁹ P. L. Cook, W. Yang, X. Liu, J. M. Garcia-Lastra, A. Rubio, and F. J. Himpsel, *J. Chem. Phys.* **134**, 204707 (2011).
- ¹⁰ I. Kröger, B. Stadtmüller, C. Kleinmann, P. Rajput, and C. Kumpf, *Phys. Rev. B* **83**, 195414 (2011).
- ¹¹ E. Rauls, W. G. Schmidt, T. Pertram, and K. Wandelt, *Surf. Sci.* **606**, 1120 (2012).
- ¹² C. Stadler, S. Hansen, I. Kröger, C. Kumpf, and E. Umbach, *Nat. Phys.* **5**, 153 (2009).
- ¹³ R. R. Lunt, J. B. Benziger, and S. R. Forrest, *Adv. Mater.* **19**, 4229 (2007).
- ¹⁴ J. K. Gimzewski, E. Stoll, and R. R. Schlittler, *Surf. Sci.* **181**, 267 (1987).
- ¹⁵ P. H. Lippel, R. J. Wilson, M. D. Miller, Ch. Wöll, and S. Chiang, *Phys. Rev. Lett.* **62**, 171 (1989).
- ¹⁶ R. Möller, R. Coenen, A. Esslinger, and B. Koslowski, *J. Vac. Sci. Technol. A* **8**, 659 (1990).
- ¹⁷ W. Mizutani, M. Shigeno, Y. Sakakibara, K. Kajimura, M. Ono, S. Tanishima, K. Ohno, and N. Toshima, *J. Vac. Sci. Technol. A* **8**, 675 (1990).
- ¹⁸ C. Ludwig, R. Strohmaier, J. Petersen, B. Gompf, and W. Eisenmenger, *J. Vac. Sci. Technol. B* **12**, 1963 (1994).
- ¹⁹ C. Dekker, S. J. Tans, B. Oberndorff, R. Meyer, and L. C. Venema, *Synth. Met.* **84**, 853 (1997).
- ²⁰ M. Kanai, T. Kawai, K. Motai, X. D. Wang, T. Hashizume, and T. Sakura, *Surf. Sci.* **329**, L619 (1995).
- ²¹ J.-Y. Grand, T. Kunstmann, D. Hoffmann, A. Haas, M. Dietsche, J. Seifritz, and R. Möller, *Surf. Sci.* **366**, 403 (1996).
- ²² Y. Maeda, T. Matsumoto, M. Kasaya, and T. Kawai, *Jpn. J. Appl. Phys.* **35**, L405 (1996).
- ²³ M. Nakamura, Y. Morita, and H. Tokumoto, *Appl. Surf. Sci.* **113/114**, 316 (1997).
- ²⁴ M. Böhringer, R. Berndt, and W.-D. Schneider, *Phys. Rev. B* **55**, 1384 (1997).
- ²⁵ M. C. Hersam, N. P. Guisinger, and J. W. Lyding, *J. Vac. Sci. Technol. A* **18**, 1349 (2000).
- ²⁶ R. Hiesgen, M. Raebisch, H. Boettcher, and D. Meissner, *Sol. Energy Mater. Sol. Cells* **61**, 73 (2000).
- ²⁷ M. Stoehr, T. Wagner, M. Gabriel, B. Weyers, and R. Möller, *Adv. Funct. Mater.* **11**, 175 (2001).
- ²⁸ X. Lu, K. W. Hipps, X. D. Wang, and U. Mazur, *J. Am. Chem. Soc.* **118**, 7197 (1996).
- ²⁹ K. W. Hipps, X. Lu, X. D. Wang, and U. Mazur, *J. Phys. Chem.* **100**, 11207 (1996).
- ³⁰ X. Lu and K. W. Hipps, *J. Phys. Chem. B* **101**, 5391 (1997).
- ³¹ R. Strohmaier, C. Ludwig, J. Petersen, B. Gompf, and W. Eisenmenger, *J. Vac. Sci. Technol. B* **14**, 1079 (1996).
- ³² M. Lackinger and M. Hietschold, *Surf. Sci.* **520**, L619 (2002).
- ³³ S. N. Magonov, H.-J. Cantow, and D. M. W. v. d. Ham, *Synth. Met.* **41–43**, 2639 (1991).

- ³⁴ A. Manivannan, L. A. Nagahara, H. Yanagi, T. Kouzeki, M. Ashida, Y. Maruyama, K. Hashimoto, and A. Fujishima, *Thin Solid Films* **226**, 6 (1993).
- ³⁵ L. A. Nagahara, A. Manivannan, H. Yanagi, M. Toriida, M. Ashida, Y. Maruyama, K. Hashimoto, and A. Fujishima, *J. Vac. Sci. Technol. A* **11**, 781 (1993).
- ³⁶ A. Manivannan, L. A. Nagahara, K. Hashimoto, and A. Fujishima, *Langmuir* **9**, 771 (1993).
- ³⁷ T. G. Gopakumar, M. Lackinger, M. Hackert, F. Müller, and M. Hietschold, *J. Phys. Chem. B* **108**, 7839 (2004).
- ³⁸ Y. F. Wang, J. Kröger, R. Berndt, H. Vázquez, M. Brandbyge, and M. Paulsson, *Phys. Rev. Lett.* **104**, 176802 (2010).
- ³⁹ Y. F. Wang, J. Kröger, R. Berndt, and W. A. Hofer, *J. Am. Chem. Soc.* **131**, 3639 (2009).
- ⁴⁰ J. Mao, H. Zhang, Y. Jiang, Y. Pan, M. Gao, W. Xiao, and H.-J. Gao, *J. Am. Chem. Soc.* **131**, 14136 (2009).
- ⁴¹ P. Jiang, X. Ma, Y. Ning, C. Song, X. Chen, J. F. Jia, and Q. K. Xue, *J. Am. Chem. Soc.* **130**, 7790 (2008).
- ⁴² A. Zhao, Q. Li, L. Chen, H. Xiang, W. Wang, Sh. Pan, B. Wang, X. Xiao, J. Yang, J. G. Hou, and Q. Zhu, *Science* **309**, 1542 (2005).
- ⁴³ Z. Li, B. Li, J. Yang, and J. G. Hou, *Acc. Chem. Res.* **43**, 954 (2010), and references therein.
- ⁴⁴ S. H. Chang, S. Kuck, J. Brede, L. Lichtenstein, G. Hoffmann, and R. Wiesendanger, *Phys. Rev. B* **78**, 233409 (2008).
- ⁴⁵ B. W. Heinrich, C. Iacovita, T. Brumme, D.-J. Choi, L. Limot, M. V. Rastei, W. A. Hofer, J. Kortus, and J.-P. Bucher, *J. Phys. Chem. Lett.* **1**, 1517 (2010).
- ⁴⁶ Y. F. Wang, J. Kröger, R. Berndt, and W. Hofer, *Angew. Chem., Int. Ed.* **48**, 1261 (2009).
- ⁴⁷ Z. H. Cheng, L. Gao, Z. T. Deng, N. Jiang, Q. Lui, D. X. Shi, S. X. Du, H. M. Guo, and H.-J. Gao, *J. Phys. Chem. C* **111**, 9240 (2007).
- ⁴⁸ Y. F. Wang, X. Ge, C. Manzano, J. Kröger, R. Berndt, W. A. Hofer, H. Tang, and J. Cerdá, *J. Am. Chem. Soc.* **131**, 10400 (2009).
- ⁴⁹ Q. M. Guo, M. Huang, Z. H. Qiu, and G. Y. Cao, *Ultramicroscopy* **118**, 17 (2012).
- ⁵⁰ K. W. Hipps and U. Mazur, *J. Porphy. Phthal.* **16**, 273 (2012).
- ⁵¹ K. Wu, Q. H. Huang, H. J. Zhang, Q. Liao, and P. M. He, *Chin. Phys. B* **21**, 037202 (2012).
- ⁵² M. C. Cottin, J. Schaffert, A. Sonntag, H. Karacuban, and R. Möller, *Appl. Surf. Sci.* **258**, 2196 (2012).
- ⁵³ F. Chen, X. Chen, L. Liu, X. Song, S. Liu, J. Liu, H. Ouyang, Y. Cai, X. Liu, H. Pan, J. Zhu, and L. Wang, *Appl. Phys. Lett.* **100**, 081602 (2012).
- ⁵⁴ J. Otsuki, *Coord. Chem. Rev.* **254**, 2311 (2010).
- ⁵⁵ A. Mugarza, R. Robles, C. Krull, R. Korytár, N. Lorente, and P. Gambardella, *Phys. Rev. B* **85**, 155437 (2012).
- ⁵⁶ N. Tsukahara, S. Shiraki, S. Itou, N. Ohta, N. Takagi, and M. Kawai, *Phys. Rev. Lett.* **106**, 187201 (2011).
- ⁵⁷ N. Papageorgiou, E. Salomon, T. Angot, J. M. Layet, L. Giovannelli, and G. L. Lay, *Prog. Surf. Sci.* **139**, 170 (2004).
- ⁵⁸ S. Yoshimoto and N. Kobayashi, *Struct. Bond* **135**, 137 (2010).
- ⁵⁹ Y. F. Wang, Y. C. Ye, and K. Wu, *J. Phys. Chem. B* **110**, 17960 (2006).
- ⁶⁰ Y. F. Wang, J. Kröger, R. Berndt, and H. Tang, *J. Am. Chem. Soc.* **132**, 12546 (2010).
- ⁶¹ R. Cuadrado, J. I. Cerdá, Y. F. Wang, X. Ge, R. Berndt, and H. Tang, *J. Chem. Phys.* **133**, 154701 (2010).
- ⁶² Y. F. Wang, X. Ge, G. Schull, R. Berndt, C. Bornholdt, F. Köhler, and R. Herges, *J. Am. Chem. Soc.* **130**, 4218 (2008).
- ⁶³ Y. F. Wang, X. Ge, G. Schull, R. Berndt, C. Bornholdt, H. Tang, F. Köhler, and R. Herges, *J. Am. Chem. Soc.* **132**, 1196 (2010).
- ⁶⁴ H. Liang, Y. He, Y. C. Ye, X. G. Xu, F. Cheng, W. Sun, X. Shao, Y. F. Wang, J. L. Li, and K. Wu, *Coord. Chem. Rev.* **253**, 2959 (2009).
- ⁶⁵ H. Liang, W. Sun, X. Jin, H. Li, J. L. Li, X. Q. Hu, B. K. Teo, and K. Wu, *Angew. Chem., Int. Ed.* **50**, 7562 (2011).
- ⁶⁶ S. U. Nanayakkara, E. C. H. Sykes, L. C. Fernandez-Torres, M. M. Blake, and P. S. Weiss, *Phys. Rev. Lett.* **98**, 206108 (2007).
- ⁶⁷ I. Fernandez-Torrente, S. Monturet, K. J. Franke, J. Fraxedas, N. Lorente, and J. I. Pascual, *Phys. Rev. Lett.* **99**, 4 (2007).
- ⁶⁸ J. Repp, F. Moresco, G. Meyer, K. H. Rieder, P. Hyldgaard, and M. Persson, *Phys. Rev. Lett.* **85**, 2981 (2000).
- ⁶⁹ F. Silly, M. Pivetta, M. Ternes, F. Patthey, J. P. Pelz, and W. D. Schneider, *Phys. Rev. Lett.* **92**, 016101 (2004).
- ⁷⁰ S. Lukas, G. Witte, and C. Wöll, *Phys. Rev. Lett.* **88**, 028301 (2002).
- ⁷¹ R. Wang, K. Hashimoto, and A. Fujishima, *Nature* **388**, 6641 (1997).
- ⁷² M. Grätzel, *Nature* **414**, 332 (2001).
- ⁷³ S. U. M. Khan, M. Al-Shahry, and W. B. Ingler, *Science* **297**, 2243 (2002).
- ⁷⁴ U. Diebold, *Surf. Sci. Rep.* **48**, 53 (2003).
- ⁷⁵ R. Schaub, E. Wahlstrom, A. Ronnau, E. Lagsgaard, I. Stensgaard, and F. Besenbacher, *Science* **299**, 377 (2003).
- ⁷⁶ R. A. Bennett, P. Stone, R. D. Smith, and M. Bowker, *Surf. Sci.* **454**, 390 (2000).
- ⁷⁷ J. A. Rodriguez, T. Jirsak, J. Liu, J. Hrbek, J. Dvorak, and A. Maiti, *J. Am. Chem. Soc.* **123**, 9597 (2001).